Electronic Supplementary Material (ESI) for ChemComm.

# Electronic Supplementary Information

# Intracavity folding of a perylene dye affords a high-affinity complex with cucurbit[8]uril

Gyan H. Aryal,[a] Khaleel I. Assaf,[b] Kenneth W. Hunter,[a] Werner M. Nau,*[b] and Liming Huang*[a]

[a]*Department of Microbiology and Immunology, School of Medicine, University of Nevada, Reno, NV 89557, USA*

[b]*Department of Life Sciences and Chemistry, Jacobs University Bremen, Campus Ring 1, 28759 Bremen, Germany*

**Table of Contents**

## 1. Experimental Section

### 1.1. General methods

Unless otherwise stated, all solvents and chemicals were purchased from Sigma Aldrich and used without further purification. Cucurbit[7]uril and cucurbit[8]uril were purchased Strem Chemicals Inc. (Newburyport, MA) and dried at 110 ºC for 24 hours before use. $^1$H- and $^{13}$C-NMR spectra were recorded on either a Varian 400 or 500 MHz spectrometer in $CDCl_3$, DMSO-$d_6$, $CF_3COOD$, $D_2O$, or a mixture of $D_2O$ and DMSO-$d_6$. MALDI-TOF spectra were recorded on a Bruker Autoflex3 Matrix Assisted Laser Desorption Ionization-Time of Flight Mass Spectrometer (MALDI-TOF MS).

UV-vis spectra were recorded with a dual-beam Perkin Elmer Lambda 950 Spectrophotometer using UV-WIN Lab version 5.1.5 software. Fluorescence spectra were acquired using a Jobin-Yvon Horiba Fluorolog 3-222 Fluorescence Spectrophometer. 1-cm quartz cuvettes or methacrylate plastic cuvettes were used for both UV-vis and fluorescence studies.

The binding constant of CB8:**PMI1** complexes as determined by fluorescence titration was calculated with a 1:1 host-guest binding model using the Origin program (OriginLab Corporation) and the equation (Int=Igh+(Ig-Igh)*(((Go-Ho-1/Kg)/2+sqrt(((Ho+Go+1/Kg)^2)/4-Ho*Go))/Go), where Ig is the fluorescence intensity of guest, Igh is the intensity of host-guest complexes, Go is the concentration of the guest, and Kg is the binding constant). The binding constant of CB8 with different guests (AD and MV) as determined by fluorescence displacement titration was calculated with 1:1:1 host-guest-competitor model using the Origin program and the equation (y=Ig+(Igh(Io,Ig,Kg,Go,Ho)-Ig)*Kg*rac(Kg,Kc,x,Go,Ho)/(1+Kg*rac(Kg,Kc,x,Go,Ho)), where Ig is the fluorescence intensity of guest, Io is the fluorescence intensity of host-guest complexes, Kg is the binding constant of host-guest complexes, Kc is the binding constant of host-competitor complexes, Go is the concentration of the guest, Ho is the concentration of the host).

Quantum yields were determined using another a previous reported water-soluble perylene monoimide as a standard (QY=0.50 in methanol).[1,2]

Lifetime measurements were performed at 25 °C using a Fluorolog-3 Fluorometer equipped with a NanoLED (492 nm), FluoroHub TCSPC, a single photon detector, and DataStation DAS6 Foundation Software. All studies were performed without purging the solutions with inert gas to remove oxygen.

## 1.2 Synthesis of PMI1

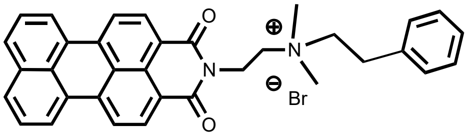

**1** (100 mg, 0.25 mmol, **1** was synthesized according to previous reported procedure and has been reported previously),[3,4] *N,N*-diisopropylethylamine (DIEA, 100 µL), and benzyl bromide (0.5 g, 2.70 mmol) were added to in toluene (5 mL) in a round bottom flask. The resulting mixture was stirred at 100 °C for 48 hrs. The reaction mixture was precipitated out with ethyl acetate and a solid was collected using a centrifuge and washed with excess ethyl acetate. The product (130 mg, 0.225 mmol, 90%) was collected after drying under vacuum at 100 °C overnight. $^1$H NMR (Varian 400 MHz, DMSO-$d_6$) δ 8.62-8.58 (m, 4H), 8.39 (d, *J* = 12 Hz, 2H), 8.1 (d, *J* = 8 Hz, 2H), 7.70 (t, *J* = 8 Hz, 2H), 7.4 (d, *J* = 4 Hz, 3H), 7.33-7.31 (m, 1H) 4.51 (t, *J* = 4 Hz, 2H), 3.73-3.69 (m, , 4H), 3.18 (s, 6H), 3.15 (t, *J* = 12 Hz, 2H); $^{13}$C NMR (100 MHz, DMSO-$d_6$) δ 163.4, 137.4, 136.6, 134.2, 133.9, 131.6, 129.4, 129.0, 127.8, 127.3, 125.1, 121.3, 64.3, 59.6, 51.2, 33.8, 28.6 ; MALDI-TOF: m/z = 497.77 $[M]^+$ (calc'd. 497.61 for $C_{34}H_{29}N_2O_2^+$).

### 1.3 Optical properties, UV-vis spectra, fluorescence spectra, fluorescence titration, binding calculation, DFT-optimized structures, and Mass spectrum

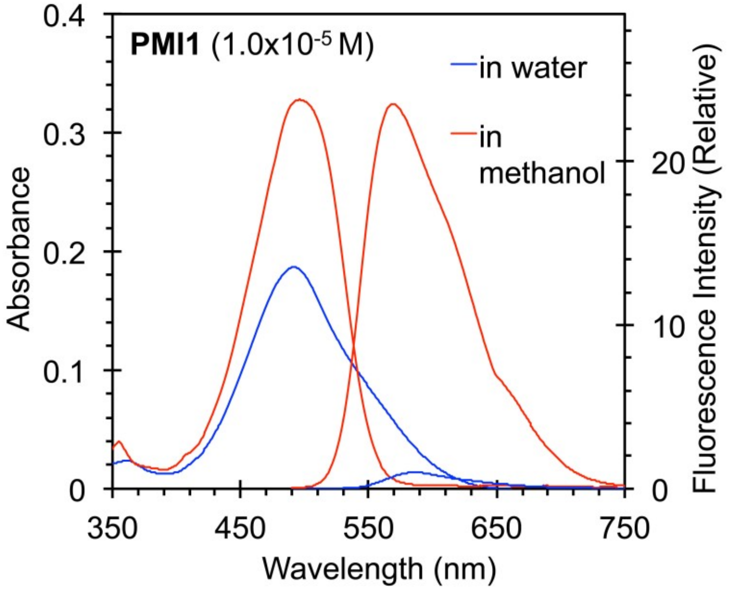

**Figure S1**. UV-vis absorbance and fluorescence emission spectra of **PMI1** ($1.0\times10^{-5}$ M) in water and methanol. The emission spectra were collected when samples were excited at 470 nm.

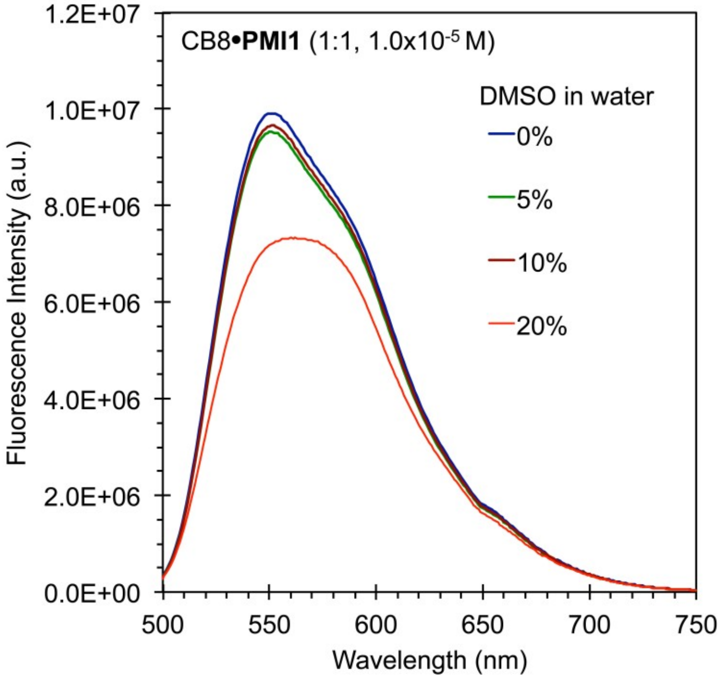

**Figure S2**. Fluorescence emission spectra of CB8•**PMI1** ($1.0\times10^{-5}$ M) in water in the presence of 0 to 20% DMSO. The emission spectra were collected when samples were excited at 470 nm.

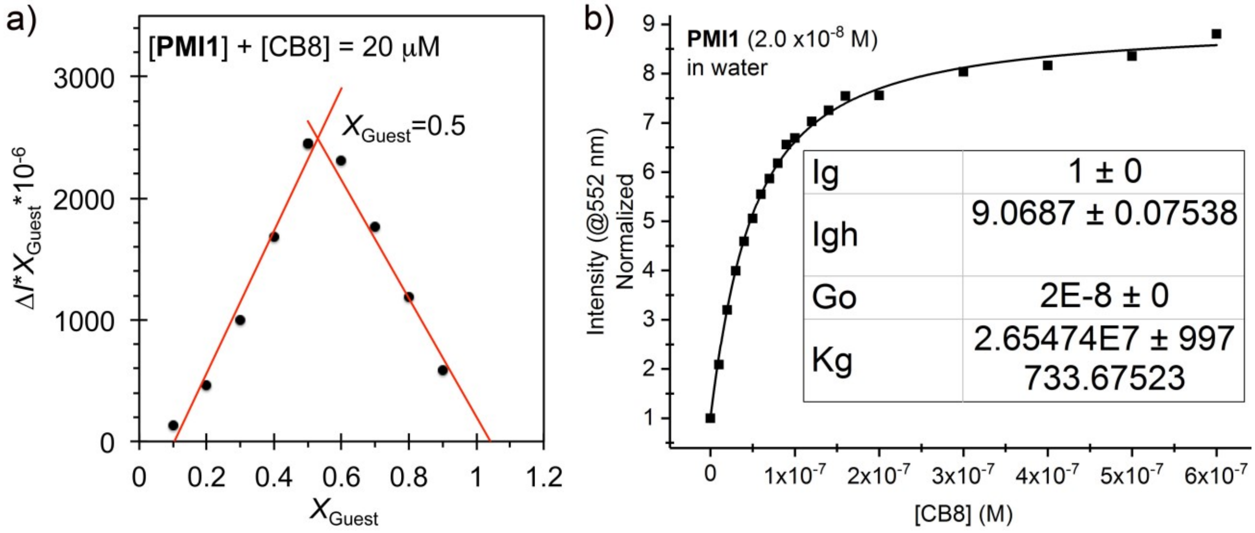

**Figure S3**. a) A Job plot for CB8•**PMI1** (the total concentration of guest **PMI1** and host CB8 was fixed at 20 μM and the fluorescence integration *I* was used in the calculation). b) The binding curve for CB8•**PMI1** (fluorescence titrations of **PMI1** in the presence of CB8 (0 to 30 equivalents) and the F.I. at 552 nm was plotted against the concentration of CB8. The red line represents the best fitting of the data to a 1:1 binding).

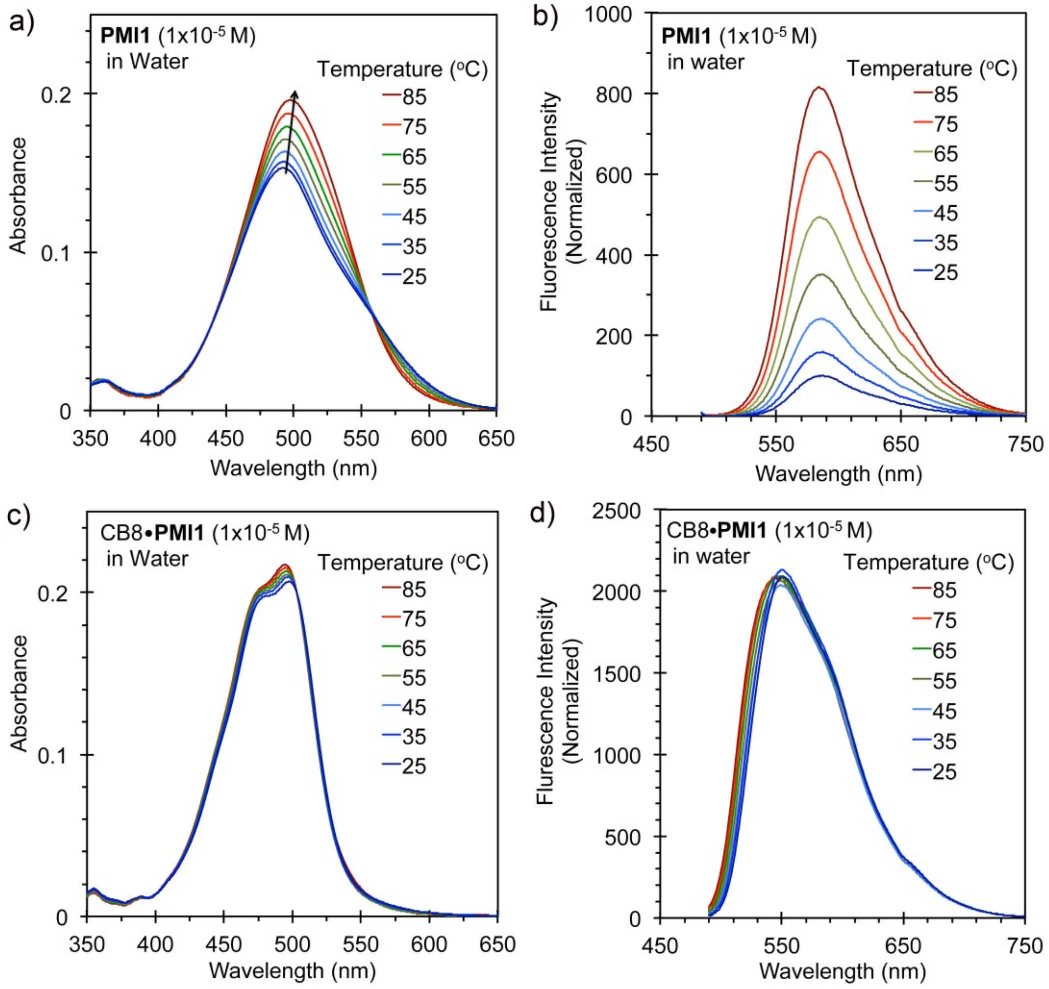

**Figure S4**. a) UV-vis absorbance and b) fluorescence emission spectra of **PMI1** (1.0×10$^{-5}$ M) in water at the temperature of 25 to 85 °C. c) UV-vis absorbance and d) fluorescence emission spectra of CB8•**PMI1** complexes (1:1, 1.0×10$^{-5}$ M) in water at the temperature of 25 to 85 °C.

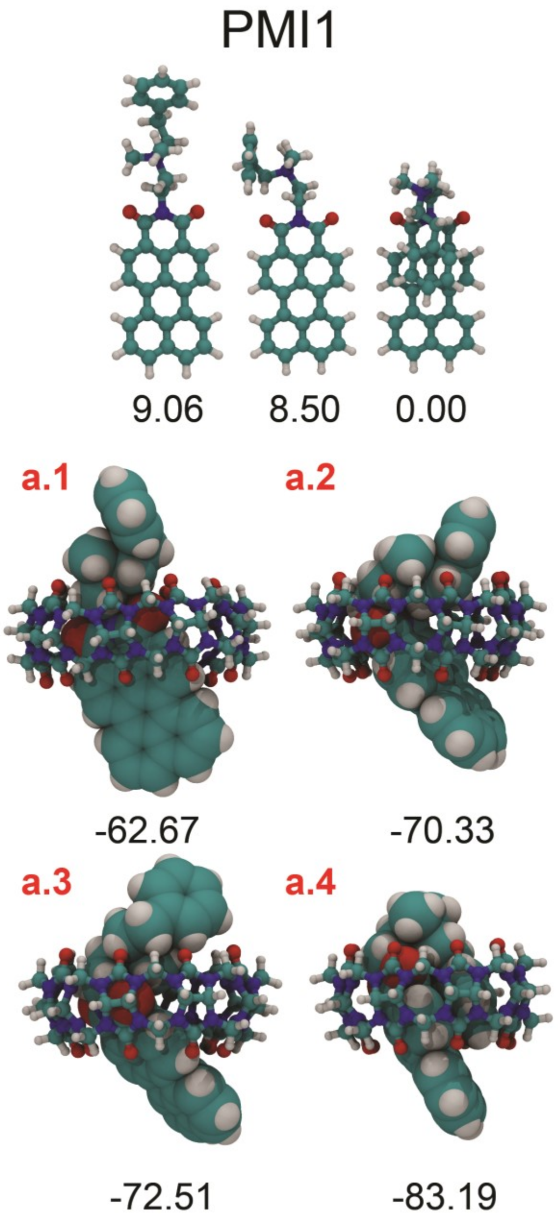

**Figure S5**. DFT-optimized structures for the different conformations of **PMI1** (top) and for the different co-conformations of the host-dye complexes (bottom) of CB8•**PMI1**. Relative energies are given below the conformations of the free dyes and the co-conformations of the complexes, all in kcal mol$^{-1}$.

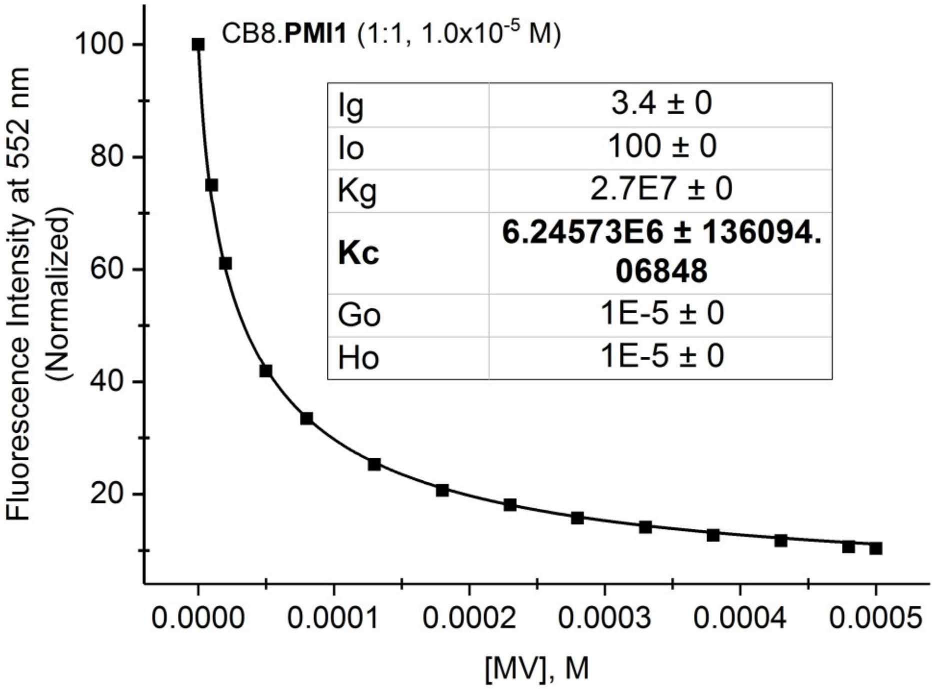

**Figure S6**. The binding curve for the displacement of CB8•**PMI1** with MV (Fluorescence titration experiment of CB8•**PMI1** (1.0×10$^{-5}$ M. 1:1) in the presence of MV and the fluorescence Intensity at 552 nm was plotted against the concentration of MV. The red line represents the best fitting of the data.)

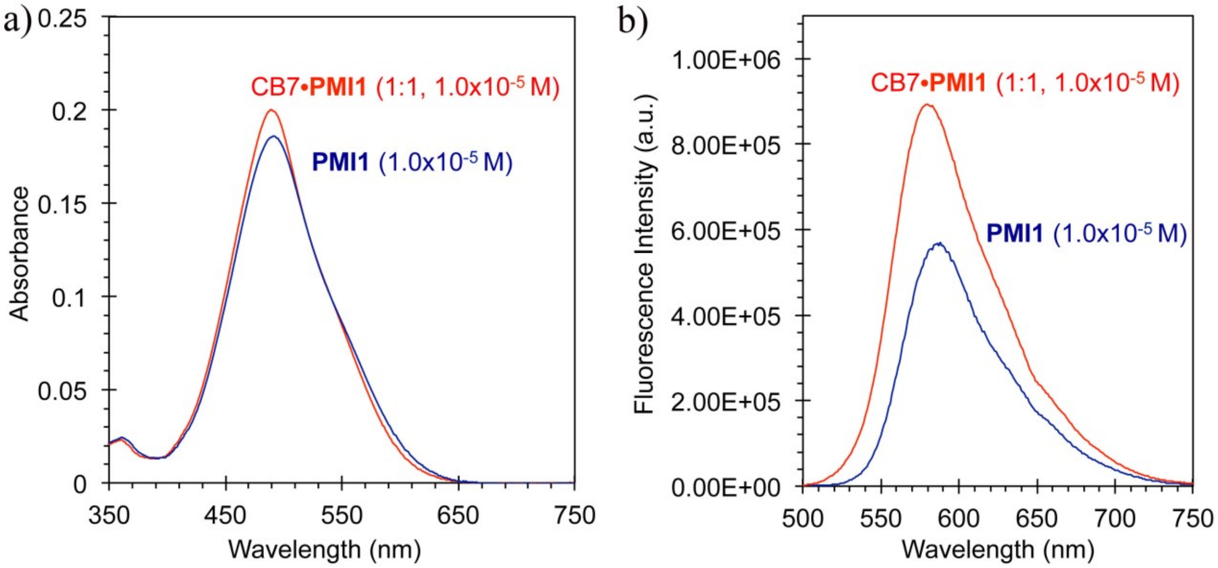

**Figure S7**. a) UV-vis absorbance and b) fluorescence emission spectra of **PMI1** (1.0×10$^{-5}$ M) in water and in the presence of 1.0 equivalent of CB7.

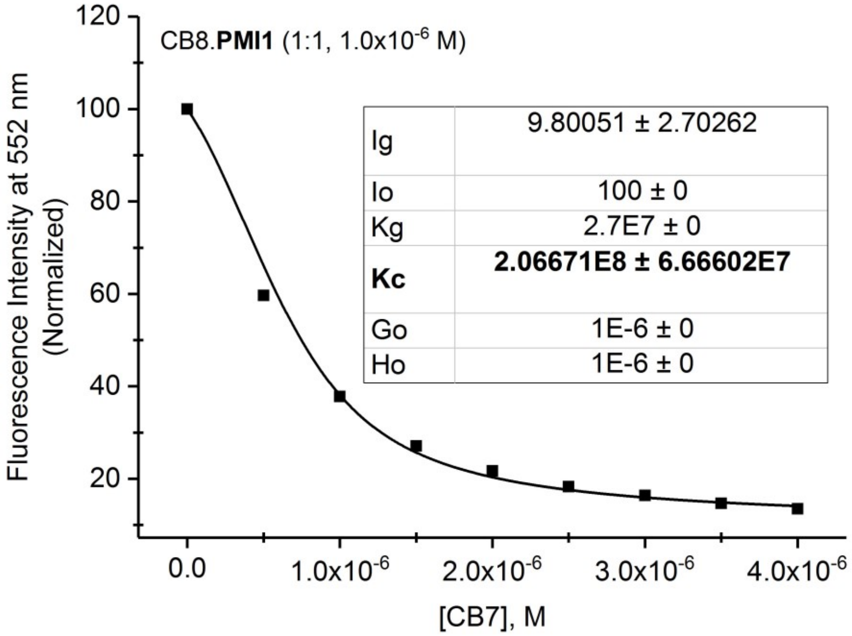

**Figure S8**. The binding curve for the displacement of CB8•**PMI1** with CB7 (Fluorescence titration experiment of CB8•**PMI1** ($1.0\times10^{-6}$ M. 1:1) in the presence of CB7 from 0 to 4.0 equivalents and the fluorescence Intensity at 552 nm was plotted against the concentration of CB7. The red line represents the best fitting of the data.)

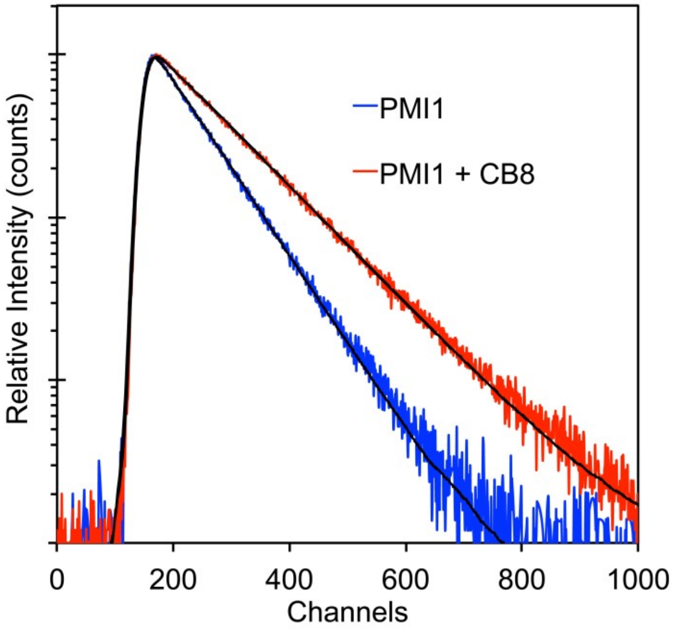

**Figure S9.** Time-correlated single photon counting fluorescence decay profiles for CB8•**PMI1** (1:1 ratio). The measurement was performed with excitation at 492 nm (NanoLED) and emission at 555 nm.

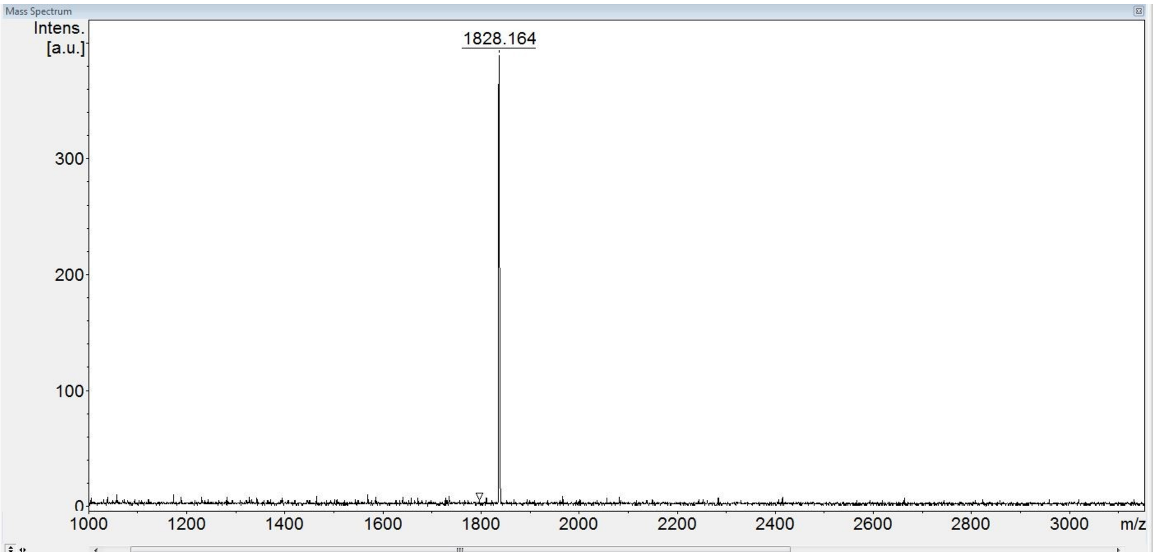

**Figure S10.** MALDI mass of CB8•**PMI1** in $H_2O$ using 2,5-dihydroxybenzoic acid as a matrix. ([CB8•**2**+H]$^{2+}$: observed mass 1828.16 Da, calculated mass1827.89 Da).

### 1.4 Quantum chemical calculations

Quantum-chemical calculations were performed with the Gaussian 09 package,[5] utilizing density functional theory (DFT) with dispersion corrected method (wB97xd) in combination with 6-31G* basis set. Different starting geometries were considered for the free guests and their host•guest complexes with CB8. Minima were characterized by the absence of imaginary frequencies.

**Table S1.** DFT-calculated (wb97xd/6 31G*) binding energies[a] in kcal mol$^{-1}$.

| CB8•**PMI1** | $\Delta E$/ kcal mol$^{-1}$ |
|---|---|
| a.1 | −76.68 (−62.67) |
| a.2 | −88.05 (−70.33) |
| a.3 | −90.04 (−72.51) |
| a.4 | −102.24 (−83.19) |

[a] Values in parentheses are with counterpoise (CP) correction for basis set superposition errors; see Figure S5 for the optimized structures.

## 1.5 NMR spectra

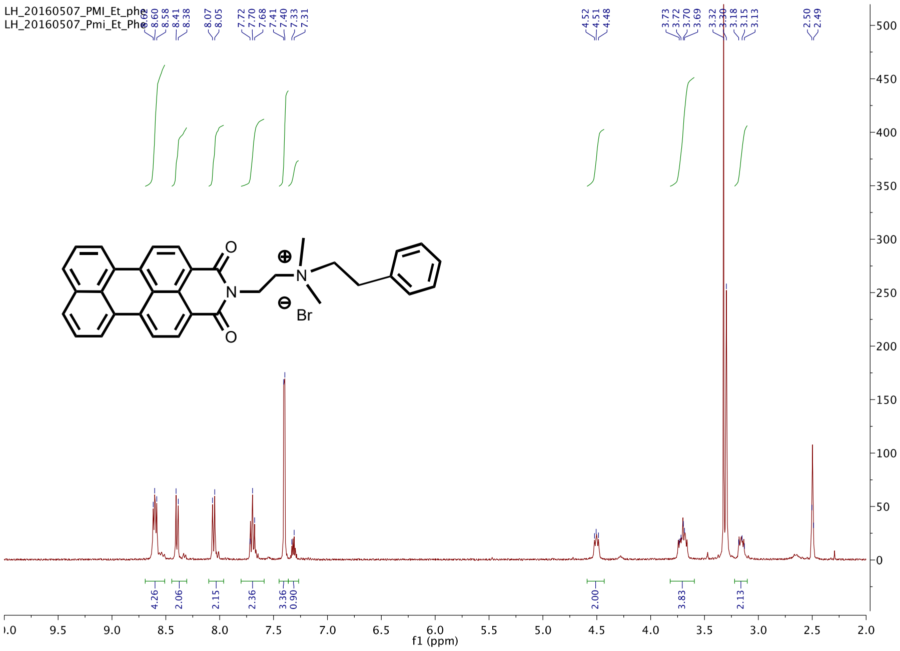

**Figure S11**. $^{1}$H-NMR of **PMI1** in DMSO-d6.

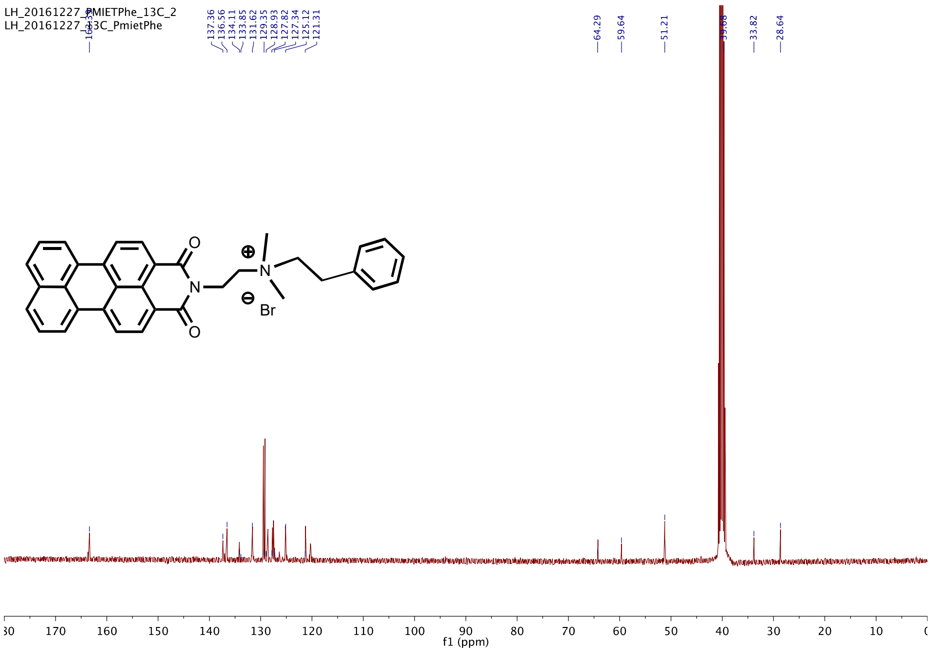

**Figure S12**. $^{13}$C-NMR of **PMI1** in DMSO-d6.

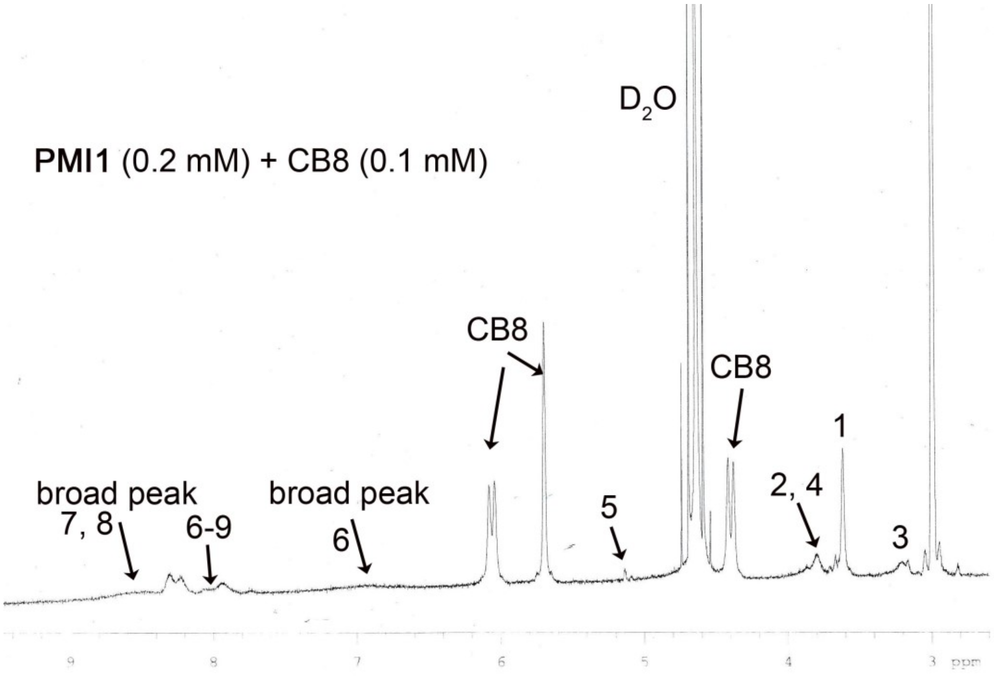

**Figure S13.** ${}^1$H-NMR spectrum of **PMI1** (0.2 mM) in the presence of 0.5 equivalent of CB8 (0.1 mM) in $D_2O$ with 10% DMSO-$d_6$.

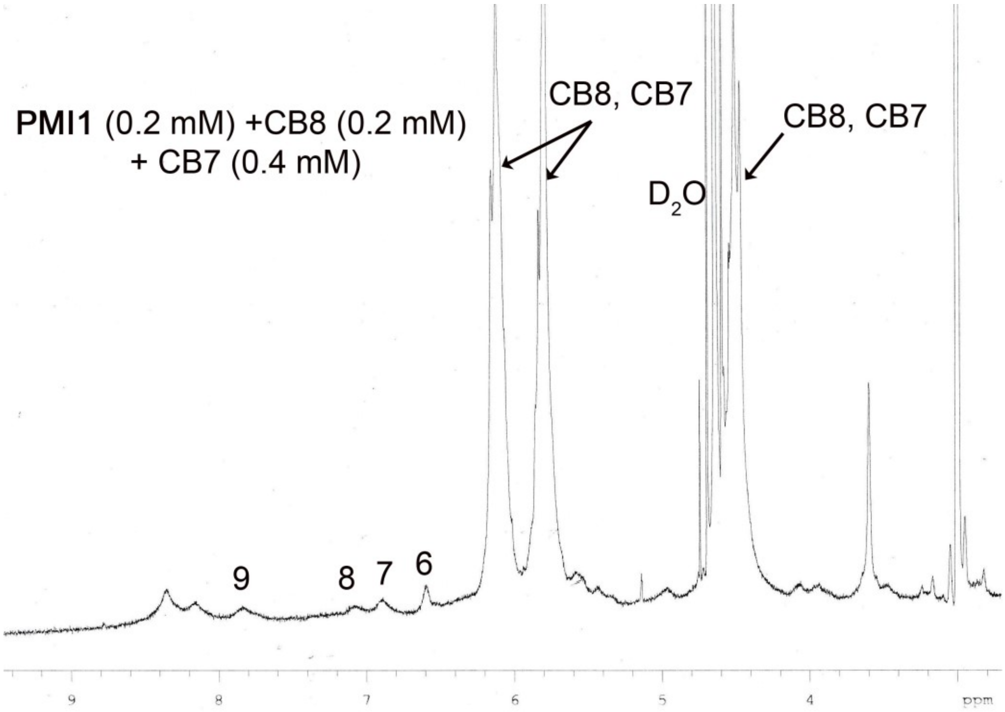

**Figure S14.** ${}^1$H-NMR spectrum of CB8•**PMI1** (0.2 mM, 0.2 mM) in the presence of 2.0 equivalent of CB7 (0.4 mM) in $D_2O$ with 10% DMSO-$d_6$.

## 1.6 References

1. L. Huang, S.-W. Tam-Chang, W. Seo and K. Rove, *Adv. Mater.,* 2007, **19**, 4149-4152.
2. L. Huang and S.-W. Tam-Chang, *J. Fluoresc.,* 2011, **21**, 213-222.
3. L. Huang, V. J. Catalano and S.-W. Tam-Chang, *Chem. Commun.,* 2007, **43**, 2016-2018.
4. G. H. Aryal, L. Huang and K. W. Hunter, *RSC Adv*., 2016, **6**, 82566-82570.
5. M. J. Frisch, G. W. T., H. B. Schlegel, G. E. Scuseria, ; M. A. Robb, J. R. C., G. Scalmani, V. Barone, B. Mennucci, ; G. A. Petersson, H. N., M. Caricato, X. Li, H. P. Hratchian, ; A. F. Izmaylov, J. B., G. Zheng, J. L. Sonnenberg, M. Hada, ; M. Ehara, K. T., R. Fukuda, J. Hasegawa, M. Ishida, T. Nakajima, ; Y. Honda, O. K., H. Nakai, T. Vreven, J. A. Montgomery, Jr., ; J. E. Peralta, F. O., M. Bearpark, J. J. Heyd, E. Brothers, ; K. N. Kudin, V. N. S., T. Keith, R. Kobayashi, J. Normand, ; K. Raghavachari, A. R., J. C. Burant, S. S. Iyengar, J. Tomasi, ; M. Cossi, N. R., J. M. Millam, M. Klene, J. E. Knox, J. B. Cross, ; V. Bakken, C. A., J. Jaramillo, R. Gomperts, R. E. Stratmann, ; O. Yazyev, A. J. A., R. Cammi, C. Pomelli, J. W. Ochterski, ; R. L. Martin, K. M., V. G. Zakrzewski, G. A. Voth, ; P. Salvador, J. J. D., S. Dapprich, A. D. Daniels, ; O. Farkas, J. B. F., J. V. Ortiz, J. Cioslowski, ; Fox, a. D. J.; Gaussian, Inc.: Wallingford CT, 2010.